

- **Short report**

## Modeling and dose calculations of a pure beta emitting $^{32}\text{P}$ coated stent for intracoronary brachytherapy by Monte Carlo code

O. Kiavar<sup>1</sup> and M. Sadeghi<sup>2\*</sup>

<sup>1</sup>Department Nuclear Engineering, Science and Research Branch, Islamic Azad University, Tehran, Iran

<sup>2</sup>Agricultural, Medical & Industrial Research School, Nuclear Science and Technology Research Institute, Karaj, Iran

**Background:** Recently, different investigators have studied the possibility of radiation therapy in restenosis prevention and have shown promising results. In this study a unique radioactive source for intra vascular brachytherapy (IVBT) was investigated. The two-dimensional dose distribution in water for a  $^{32}\text{P}$  IVBT stent has been calculated. The pure beta emitter source  $^{32}\text{P}$  has been coated on Palmaz-Schatz stent. The dosimetric parameters required by the AAPM TG-60 formalism are discussed and calculated. **Materials and Methods:** The dose distribution of the activated stent was determined by Version 4C of the (MCNP) Monte Carlo radiation transport code in water and it was verified by TG-60 experimental results. Dosimetric parameters such as anisotropy function,  $F(r, \theta)$ , and the radial dose function,  $g_L(r)$ , around the Palmaz-Schatz stent at distances from 0.18 to 0.9 cm have been calculated. The Palmaz-Schatz stent with 3.5 mm external diameter and 14 mm length is coated with a thin layer of  $^{32}\text{P}$ . **Results:** The Monte Carlo calculated dose rate at the reference point is found to be 17.85 Gy. The results were compared with previously published paper for an actual same source. The difference between these two data sets is in acceptable range. There were almost little differences (less than 0.05%) in values among them. **Conclusion:** The dosimetry parameters such as, geometry function,  $G(r, \theta)$ , anisotropy function,  $F(r, \theta)$  and radial dose function,  $g(r)$ , were determined according to TG-60 protocols and listed in tabular format. High dose variants were visible near the  $^{32}\text{P}$  stent surface, but these values decreased with depth in vessel layers rapidly. There are an acceptable agreement between the calculated data in this study and other published data for the same source. However, the observed differences between the calculated and measured values could be explained by the measurement uncertainty and the geometry modeling during the simulations. **Iran. J. Radiat. Res., 2012; 9(4): 257-263**

**Keywords:** Coronary stent, radioactive stent, intravascular brachytherapy,  $^{32}\text{P}$ , MCNP4C.

### INTRODUCTION

Percutaneous transluminal coronary angioplasty (PTCA) is currently one of the most common treatments for obstructive coronary artery disease.<sup>(1)</sup> The long term effectiveness of angioplasty is limited by vessel renarrowing called restenosis, which occurs within six months following the procedure. Restenosis often requires additional treatment, including angioplasty or bypass surgery, in 20% to 30% of patients<sup>(2)</sup>. Coronary stenting with expandable metallic scaffolding devices is the first mechanical treatment that has been shown to reduce restenosis in randomized clinical trials. Although recoil and remodeling effects are greatly reduced, neointimal thickening due to proliferation is actually enhanced<sup>(3-5)</sup>. Pharmacological efforts to reduce neointimal proliferation have thus far been fruitless in patients<sup>(6-7)</sup>. About 10 years ago, a number of investigators began to study the potential use of ionizing radiation for reducing neointimal proliferation<sup>(8)</sup>. Intravascular radiation therapy with radioactive stent has now shown be promising in several animal models, hence conflicting results have also been reported<sup>(9-10)</sup>. The efficiency of radiation treatment for restenosis has yet to be determined in human. The

#### \*Corresponding author:

Dr. Mahdi Sadeghi,  
Nuclear Science and Technology Research Institute  
P.O. Box 31485/498, Karaj, Iran.

Fax: +98 261 4464055

E-mail: msadeghi@nrcam.org

challenge of intravascular delivery of radiation is to safely deliver a highly localized dose to the arterial wall including the intima, media and possibly the adventitia<sup>(11)</sup>. One important problem worth to be noted about the drug eluting stent is that it is possible for radioactive material to enter into the vessel wall, or be carried away in the bloodstream after stent implantation<sup>(12)</sup>.

Due to the high dose gradient at short distances from a radioactive stent, traditional dosimetry is difficult or even impossible and there is some few published data on the dose distribution within the arterial wall<sup>(13)</sup>. Monte Carlo dose calculations, when carefully validated, provide the highest level of accuracy for dose calculation in treatment planning.

In this paper, a brachytherapy source, pure beta emitting coronary stent (Palmazschatz stent coated by <sup>32</sup>P) was discussed and was dedicated to the Monte Carlo method to calculate the dosimetric parameters by MCNP4C code, for the <sup>32</sup>P brachytherapy source. The main aim of this study was to evaluate the dosimetric parameters of the <sup>32</sup>P stent according to TG-60<sup>(13)</sup> recommendation. The Monte Carlo calculated results in this study have been compared with the reported data by Carter *et al.*<sup>(12, 14)</sup> for the same type of the source.

## MATERIALS AND METHODS

### Source description

The physical parameters of the stent, defined in TG-60 were used to model the stent<sup>(15)</sup>. The brachytherapy source The source was made of stainless steel [Cr (17%), Ni (13%), Mo (2.5%), Fe (64.5%), Si (1%), Mn (2%)] and coated with a thin layer (1  $\mu$ m) of radioactive <sup>32</sup>P.<sup>(16)</sup> The source has a pre-expanded nominal length of 14 mm with an external diameter of 3.5 mm after expansion which is located in the martensitic crystalline phase at body temperature. According to TG-60 recommendation source activity is 1.0  $\mu$ Ci.

### Monte Carlo evaluation

The Monte Carlo N-Particle code (MCNP version 4C) was used for the dose-rate simulations<sup>(17)</sup>. Figure 1 shows a schematic diagram of the stent. For the dose calculation, the interstitial stent was surrounded by the cylindrical water phantom of 1.6 cm high and 1.0 cm in diameter. To avoid surface interrupting in MCNP new cylindrical stent geometry, with the net surface, very similar stents was simulated (figure 1). The detectors were defined in form of shells with 0.1 mm thickness and 0.2 mm height from  $r = 0.18$  to 0.9 cm in 0.2 mm increment away from the source along the longitudinal axis. Particle fluxes and energy deposited tallies, F4 and \*F8 respectively were applied to calculate kerma and the net energy (MeV) deposited in the detectors around the source in this study.

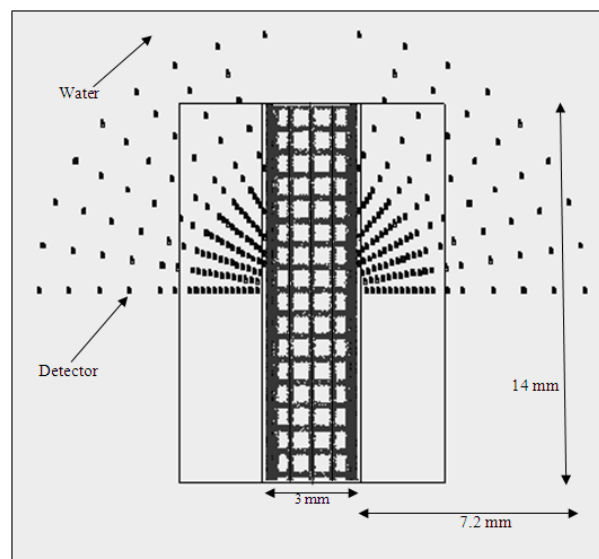


Figure 1. The geometry simulation of stent and defined detectors by MCNP4C (vertical cross section).

The calculations were performed up to  $2 \times 10^7$  histories with this number of histories, the statistical uncertainty at  $r \leq$  is less than 0.4%. The dose rate was then calculated by multiplying the dose per starting particle, the source activity (dps) and <sup>32</sup>P beta emission intensity. The delivered dose was calculated by integrating dose rate during 28 days for a 1.0  $\mu$ Ci stent,

based on the experimental measurements<sup>(13)</sup>.

### AAPM TG-60 parameters

The main purpose in this article was to determine the parameters, described in TG-60 protocol. The detectors were defined at polar angles of  $0^\circ$ – $90^\circ$  in  $10^\circ$  increments and at radial distances of  $r = 0.18, 0.2, 0.22, 0.24, 0.26, 0.28, 0.3, 0.32, 0.34, 0.36, 0.38, 0.4, 0.45, 0.5, 0.6, 0.7, 0.8$  and  $0.9$  cm. F4 tally was employed to calculate  $G(r,\theta)$ , with the mass densities of all materials within the entire computational geometry set equal to zero so there were no interaction and particles streamed through the stent and phantom geometry<sup>(18,19)</sup>. According to TG-43U1 protocol for calculating  $G(r,\theta)$  the source supposed to be line source.<sup>(20)</sup>

The anisotropy function,  $F(r,\theta)$ , accounts for the angular dependence of beta absorption and scatter. In order to calculation of the anisotropy function, the \*F8 tally was used to obtain dose per particle in detectors by using beta emitters formula for lattice cylindrical source according to (equation 1)<sup>(21, 22)</sup>

$$F(r, \theta) = \frac{\dot{D}(r, \theta) G_L(r, \theta_0)}{\dot{D}(r, \theta_0) G_L(r, \theta)} \quad (1)$$

The radial dose function,  $g(r)$ , accounts for radial dependence of beta absorption and scatter in the medium along the transverse axis. According to the methodology described in TG-60,  $g(r)$  was calculated by using line-source geometry for the stent by the following equation (equation 2)<sup>(23)</sup>

$$g_x(r) = \frac{\dot{D}(r, \theta_0) G_L(r_0, \theta_0)}{\dot{D}(r_0, \theta_0) G_L(r, \theta_0)} \quad (2)$$

Where  $D(r,\theta)$ = dose in water at the point of  $r$  and  $\theta$  angle,  $G(r,\theta)$ = geometry factor resulting from spatial distribution of the radioactivity within the source. The reference point for intravascular brachytherapy calibration for beta sources should be  $r_0=2$  mm and  $\theta_0=\pi/2$ <sup>(22)</sup>.

## RESULTS AND DISCUSSION

Table 1 lists absolute dose rates per unit activity along the stent transverse axis calculated in this work using the MCNP4C code. For the purpose of comparison, the measured values obtained by Carter *et al.*<sup>(14)</sup> using radiochromic film are also presented. From table 1 it is seen that, the dose decreases with increased radial distance from the stent surface.

The dose distributions for  $1 \mu\text{Ci}$  stent over 28 days have been calculated and the results compared with the measured values published in TG-60 at three selected points (table 2). The sharp decrease in dose beyond the active length of the source in the longitudinal (source axis) direction was also prevalent due to the short beta range of the  $^{32}\text{P}$  betas. The differences between the measured and calculated values vary by less than 4% at  $r \leq 2.5$  mm, caused by the usual errors which occur in experimental measurement due to inadequate energy response. Due to the limited penetration depth of the beta particles, as the distance increases the difference between these two data set increases and reaches about 30% at  $r = 3.5$  mm. These differences were due to the prevalent errors which occurred in experimental measurements and the short range of beta particles.

Figure 2 demonstrates the dose fall-off curve relative to the radial distances from the source. The dose related to the center of source decreased quickly from 18 Gy to 0.012 Gy as the distance increased from 0.2 cm to 0.4 cm, respectively. The  $G(r,\theta)$  parameters were calculated by applying F4 tally fluctuations for a cylindrical source analytically and the results are tabulated in table 3. The anisotropy function,  $F(r,\theta)$ , accounts for the variation of dose distribution around the source as a function of distance and angle from the center of the source. The values are presented in table 4. The steep dose gradient in the radial direction caused high values of  $F(r,\theta)$  encountered at shallow angles and further

distances from the source center.

The calculated line source radial dose function,  $g_L(r)$ , for the stent are presented in table 5.  $g_L(r)$ , was calculated in 0.02 cm increments from  $r = 0.03$  to 0.25 cm and in 0.05 increments from  $r = 0.25$  to 0.65 cm and. Figure 3 depicts the radial dose functions curve with respect to the distances from the center of stent. Calculated  $g_L(r)$  in water was fit to a third order polynomial function yielded the following relationship

(distance  $r$  is expressed in cm):

$$g(r) = \exp(a_0 + a_1r + a_2r^2 + a_3r^3),$$

with parameters  $a_0 = 0.5452$ ,  $a_1 = -0.3564$ ,  $a_2 = 0.0536$ ,  $a_3 = -0.0084$ .

Figure 4 shows the iso-dose curves determined from MCNP simulation for the  $^{32}\text{P}$  stent in transverse plan. As shown in figure 4, the iso-dose curves of the  $^{32}\text{P}$  stent, shows an isotropic dose distribution around the source.

In this work, we have calculated the 2D dose distribution for a  $^{32}\text{P}$  IVBT source stent in water using the MCNP4C Monte Carlo code. The dose parameters required by the AAPM TG-60 formalism are discussed and calculated based on the 2D dose

**Table 1.** Dose calculation of  $^{32}\text{P}$  stent in water by the activity of 1.0  $\mu\text{Ci}$ .

Distance from Center (cm)	MCNP4C Calculated dose (Gy)
0.18	22.83
0.20	17.85
0.22	14.20
0.24	11.35
0.26	8.79
0.28	6.64
0.30	4.72
0.32	3.60
0.34	2.71
0.36	1.90
0.38	1.01
0.40	0.49
0.45	0.10
0.50	0.009
0.60	0.008
0.70	0.007
0.80	0.005
0.90	0.0003

**Table 2.** Dose comparison at three selected points between MCNP4C (calculated by present work) and experimental results.

Distance from center (cm)	Dose (Gy)	
	Measurement <sup>a</sup>	MCNP4C <sup>b</sup>
0.20	18.0	17.85
0.25	9.7	10.07
0.35	3.3	2.31

<sup>a</sup> Reference 12.

<sup>b</sup> Present work.

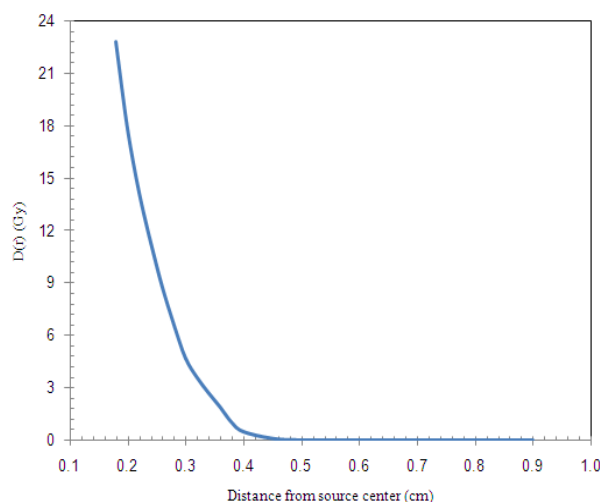


**Figure 2.** Dose fall-off of 1.0  $\mu\text{Ci}$   $^{32}\text{P}$  stent in water for 28 days (Gy).

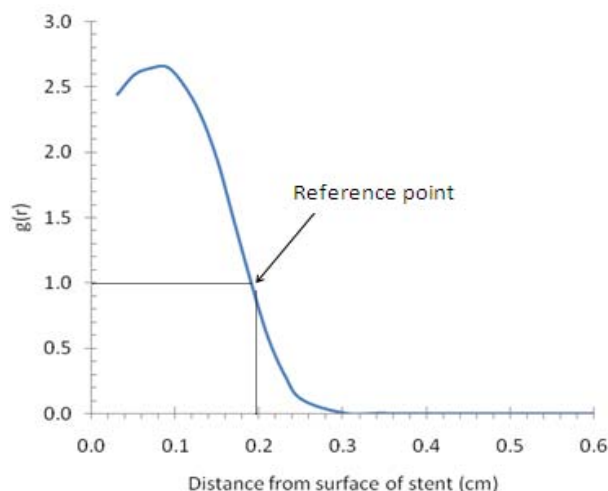


**Figure 3.** Radial dose function curve,  $g(r)$ , for  $^{32}\text{P}$  stent.

distribution. As results of the study indicate dose distribution for the beta source stent studied, is uniform along the axial direction of the stent. However, only the practical clinical trials exactly will answer the questions of whether or not radioactive stents reduce restenosis in human arteries and what activities and doses are optimal for achieving this reduction. The calculated results were in good agreement with previously published data. The results show that,  $^{32}\text{P}$  stent with  $1.0 \mu\text{Ci}$  activity, can deliver about 18 Gy dose value to 0.2 cm thick vessel wall as well as measured values. As beta particles have low range and deposit their energy in small distances through the vessel wall, this method has very low side effect on the surrounded tissues.

The subject that the isodose curves surrounding the stent at vessel wall are significantly homogeneous is considerable.

Also, matching the experimental measurements and calculated results would

help us to have more reliable treatment, but still much more investigations and human clinical experiments are needed to improve the safety of this brachytherapy sources.

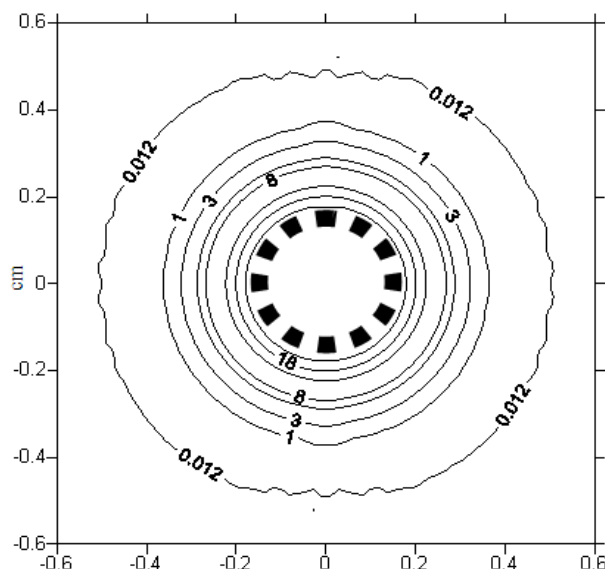


Figure 4. Isodose curves of  $1.0 \mu\text{Ci}$   $^{32}\text{P}$  stent in 28 days for treatment planning (Gy).

Table 3. Geometry function of  $^{32}\text{P}$  stent in water, Calculated by MCNP4C ( $1/\text{cm}^2$ ).

Distance from center (cm)	$G(r,\theta)$								
	10°	20°	30°	40°	50°	60°	70°	80°	90°
0.18	—	—	—	—	—	1.712	1.309	1.173	1.156
0.2	—	—	—	—	1.523	1.237	1.056	0.968	0.945
0.22	—	—	—	—	1.299	1.014	0.889	0.825	0.811
0.24	—	—	—	1.576	1.096	0.879	0.771	0.723	0.705
0.26	—	—	—	1.288	0.943	0.771	0.685	0.636	0.625
0.28	—	—	—	1.121	0.833	0.688	0.610	0.569	0.559
0.3	—	—	—	0.986	0.738	0.617	0.549	0.516	0.504
0.32	—	—	1.456	0.872	0.667	0.559	0.496	0.469	0.459
0.34	—	—	1.238	0.785	0.605	0.509	0.455	0.427	0.418
0.36	—	—	1.107	0.716	0.550	0.467	0.416	0.391	0.384
0.38	—	—	0.988	0.651	0.505	0.427	0.383	0.361	0.355
0.4	—	—	0.889	0.598	0.467	0.394	0.354	0.334	0.328
0.45	—	1.493	0.708	0.487	0.383	0.327	0.295	0.278	0.273
0.5	—	1.151	0.574	0.403	0.321	0.275	0.249	0.235	0.233
0.6	—	0.665	0.383	0.282	0.231	0.201	0.184	0.176	0.174
0.7	—	0.367	0.259	0.204	0.171	0.153	0.141	0.136	0.134
0.8	—	0.222	0.180	0.151	0.132	0.119	0.111	0.108	0.106
0.9	0.170	0.152	0.132	0.116	0.104	0.096	0.090	0.087	0.086

**Table 4.** Anisotropy function of <sup>32</sup>P stent in water, Calculated by MCNP4C.

Distance (cm)	F(r,θ)								
	10°	20°	30°	40°	50°	60°	70°	80°	90°
0.18	-	-	-	-	-	0.854	0.940	0.979	1
0.20	-	-	-	-	0.815	0.909	0.965	0.988	1
0.22	-	-	-	-	0.866	0.956	0.996	1.006	1
0.24	-	-	-	0.796	0.939	0.998	1.016	1.002	1
0.26	-	-	-	0.912	1.039	1.069	1.056	1.024	1
0.28	-	-	-	1.078	1.180	1.169	1.111	1.028	1
0.30	-	-	-	1.344	1.408	1.326	1.182	1.043	1
0.32	-	-	1.491	1.856	1.862	1.618	1.311	1.081	1
0.34	-	-	2.351	2.774	2.591	2.058	1.487	1.107	1
0.36	-	-	4.345	4.829	4.126	2.896	1.796	1.167	1
0.38	-	-	8.937	9.497	7.283	4.359	2.184	1.223	1
0.40	-	-	25.600	25.388	17.452	8.292	3.127	1.368	1
0.45	-	684.653	904.269	711.175	302.677	60.918	6.939	1.033	1
0.50	-	2540.446	2953.391	1635.821	278.237	9.779	1.464	0.985	1
0.60	-	2572.896	2023.674	252.510	0.955	1.109	1.167	0.900	1
0.70	-	1076.511	421.636	1.033	0.849	0.711	0.626	0.548	1
0.80	-	372.459	26.393	0.467	0.717	0.856	1.308	0.943	1
0.90	6.202	5.014	1.045	0.753	0.495	0.468	0.733	0.738	1

**Table 5.** Radial dose function values of the <sup>32</sup>P stent in water, Calculated by MCNP4C.

Distance (cm)	g(r)
0.03	2.439
0.05	2.592
0.07	2.643
0.09	2.651
0.11	2.509
0.13	2.281
0.15	1.928
0.17	1.460
0.19	1.004
0.21	0.582
0.23	0.294
0.25	0.107
0.30	0.003
0.35	0.001
0.45	0.001
0.55	0.002
0.65	0.002

**REFERENCES**

- Rogers C, Groothuis A, Toegel G, Stejskal E, Kamath KR, Seifert P, Hesselberg S, Delaney R, Edelman ER. (2000) Paclitaxel release from inert polymer material-coated stent curtails coronary in-stent restenosis in pigs (Abstr). *Circulation*, **102**: 11-566.
- US Directional Coronary Atherectomy Investigator Group (1990) Restenosis following directional coronary atherectomy in a multicenter experience. *Circulation*, **82**: 69-79.
- Golombek MA, Heise S, Schloesser K, Schuessler B (2003) Intravascular brachytherapy with radioactive stents produced by ion implantation. *Nuc Instrum Meth Phys Res*, **206**: 495-500.
- Kim HS, Chan RC, Kollum M, Au A, Tio FO, Yazdi HA, Ajani AE Waksman R (2001) Effects of <sup>32</sup>P radioactive stents on in-stent restenosis in a double stent injury model of the porcine coronary arteries. *Int J Radiat Oncol Biol Phys*, **51**: 1058-1063(6).
- Mintz GS, Pichard AD, Kent K, Satler LF, Popma JJ, Wong SC, Painter JA, Deforty D, Leon MB (1995) Endovascular stents reduce restenosis by eliminating geometric arterial remodeling: a serial intravascular ultrasound study. *J Am Coll Cardiol*, **35(A)**: 701-705.
- Schwartz RS, Koval TM, Edwards WD, Camrud AR, Bailey K, Browne RK, Vlietstra RE, Holmes DR (1992) Effect of external beam irradiation on neointimal hyperplasia after experimental coronary artery injury. *J Am Coll Cardiol*, **19**: 1106-1113.
- Ellis SG, Roubin GS, Wilentz J, Douglas JS, King III SB (1989) Effect of 18 to 24 hour heparin administration for prevention of restenosis after uncomplicated coronary angioplasty. *Am Heart J*, **41**: 777-782.

8. Wexberg P, Kirisits C, Gyöngyösi M, Gottsauner-Wolf M, Ploner M, Pokrajac B, Pötter R, Glogar D (2002) Vascular morphometric changes after radioactive stent implantation: a dose-response analysis. *J Am Coll Cardiol*, **39**:400-407.
9. He GJ, Gao QY, Xu SH, Gao H, Jiang T, Dai XW, Ma K (2006)  $^{103}\text{Pd}$  radioactive stent inhibits biliary duct restenosis and reduces smooth muscle actin. *Hepatobiliary Pancreat Dis Int*, **5**: 595-598.
10. Ilkay E, Tirikli L, Ozercan I, Yavuzkir M, Karaca I, Rahman A, Arslan N (2006) Oral Mycophenolate Mofetil Prevents In-Stent Intimal Hyperplasia Without Edge Effect. *Angiology*, **57**: 577-584.
11. Ettenson DS, Edelman ER (2000) *Local drug delivery: an emerging approach in the treatment of restenosis*. *Vascular Medicine*, **5**(2): 97-102.
12. Prestwich WV (1996) Analytic representation of the dose from a  $^{32}\text{P}$  coated stent. *Med Phys*, **23**: 9-13.
13. Sadeghi M, Enferadi M, Shirazi A (2010) External and internal radiation therapy: Past and future directions. *J Can Res Therapeutics*, **6**:239-48.
14. Carter A, and Lair J.R (1996) Experimental results with endovascular irradiation via a radioactive stent. *Int J Radiat Oncol Biol Phys*, **36**: 796-803.
15. Nath R, Amols H, Coffey C, Duggam D, Jani S, Li Z, Schell M, Soares C, Whiting J, Cole P, Crocker I, Schwartz R (1999) Intravascular brachytherapy physics: report of the AAPM Radiation Therapy Committee Task Group No. 60. *Med Phys*, **26**: 119-52.
16. Uniform Tubes-Europe. <http://www.uniformtubes.co.uk/>.
17. Briesmeister JF (2000) MCNP-4C A General Monte Carlo N-Particle Transport Code System—Version 4C. *Los Alamos National Laboratory, Louisiana*.
18. Raisali GH, Ataenia V, Shahvar A, M. Ghonchehnazi GH (2008) Determination of Dosimetric Parameters of the Second Model of Pd-103 Seed Manufactured at Agricultural, Medical and Industrial Research School IR. *Med Phys*, **5**: 9-20.
19. Saidi P, Sadeghi M, Shirazi A, Tenreiro C. (2010) Monte Carlo calculation of dosimetry parameters for the IR08- $^{103}\text{Pd}$  brachytherapy source. *Med Phys*, **37**: 2509-15.
20. Rivard MJ, Coursey BM, DeWerd LA, Hanson WF, Huq MS, Ibbott GS, Mitch MG, Nath R, and Williamson JF (2004) Update of AAPM task group no. 43 report: a revised AAPM protocol for brachytherapy dose calculations. *Med Phys*. **31**, 633-74.
21. Simpkin DJ and Mackie TR (1990) EGS4 Monte Carlo determination of the beta dose kernel in water. *Med Phys*, **17**: 179-186.
22. Saedghi M, Kiavar O, Hosseini SH, Fatehi R, Tenreiro C (2011) Cyclotron production and parameters calculation of  $^{48}\text{V}$  Nitinol stent for renal arteries in brachytherapy. *Journal of Radioanalytical and Nuclear Chemistry*. DOI: 10.1007/s10967-011-1138-3
23. Sadeghi M, Raisali GH, Hosseini SH, Shahvar A (2008) Monte Carlo calculations and experimental measurements of dosimetric parameters of the IRA- $^{103}\text{Pd}$  brachytherapy source. *Med Phys*, **35**: 1288-1294.

